Supporting Information

Responsive drop method: Quantitative *in-situ* determination of surfactant effectiveness using reconfigurable Janus emulsions

Saveh Djalali, Bradley D. Frank, and Lukas Zeininger*

Department of Colloid Chemistry, Max Planck Institute of Colloids and Interfaces, Am Muehlenberg 1, 14476 Potsdam, Germany

Table of Contents

1. Materials and Methods

1.1 Chemicals

All chemicals listed herein were used as received without further purification. Sodium dodecyl sulfate (99%, Sigma Aldrich), Zonyl FS-300 (40% solid in water, ABCR), Brij 58 (Sigma Aldrich), Tween 20 (Sigma Aldrich), Trition X-100 (eurobio), CTAB (99%, Sigma Alrich), AOT (98%, Sigma Aldrich), Sudan Red 7B (Sigma Aldrich), n-heptane (Fluka Chemika), perfluorodecalin (98% *cis* and *trans*, ABCR).

1.2 Instruments

NMR spectra were recorded using a Bruker Advance 400 MHz NMR spectrometer. The Lamp Spectra of the UV- and Blue light source were measured with an optical spectrometer from Avantes (StarLine, AvaSpec-ULS2048CL-EVO-RS) which was connected to an optical fibre from ThorLabs (diameter: 400 µm). For the measurements with the amphiphilic light-responsive azo-surfactant AzoTAB the complex emulsions have been irradiated until the droplets topology reached a constant state. As UV-light source we used a UV lamp from Herolab GmbH (Typ NU-4, 220 Volt, 2x4 Watt) with a wavelength of $\lambda = 366\,nm$. As blue-light source we used a custom designed LED with a wavelength of $\lambda = 461\,nm$ and a power of 74.6 mW/cm^2.

1.3 Imaging and Microscopy

For the in-situ observation of the complex emulsions and the determination of the Contact angles we used a custom designed side-view setup which was equipped with a variable zoom, composed of two tube 200 mm tube lenses and Olympus planar optical microscopy lenses. The apparatus was connected to an area scan CCD camera from HIKVision. For imaging monolayers we used generic cavity slides.

For lateral imaging of droplet morphologies glass slides with a thin cavity of 200 µm were used. First, droplets were placed on the center of the glass slide and covered with a thin glass slide. Then, the slide was brought into an upright position causing the droplets to float to the bottom of the cavity by gravity. In this setup we avoid a squishing or stacking of droplets with diameters in the range of 100-150 µm.

1.4 Image-processing algorithm

Computational contact angle determination was undertaken with a custom-written Matlab script (v2019b) utilizing the image processing toolbox. Utilizing high-contrast side-view optical micrographs containing multiple droplets of similar size in a plane. Vertically aligned droplets are first separated from the main image utilizing edge detection. Separated droplets are then processed on a case-by-case basis to detect the internal interface. For droplets where the radius of the droplet and the radius of the circle fit to the internal curvature are similar, circle pairs are used for their center point and intersection for each droplet. For cases of near-Janus droplets, where Rdroplet >> Rcurvature, blob detection is used to separate the internal interface from the droplet, three points defining the curvature are used to fit a circle, its centerpoint, and intersection. For either case, with the detected circle centerpoint and intersection, the law of cosines is used to determine the resulting contact angle.[1] A proof of concept demonstration of this concept is provided: https://github.com/brdfrnk/Complex-Droplet-Contact-Angles/.

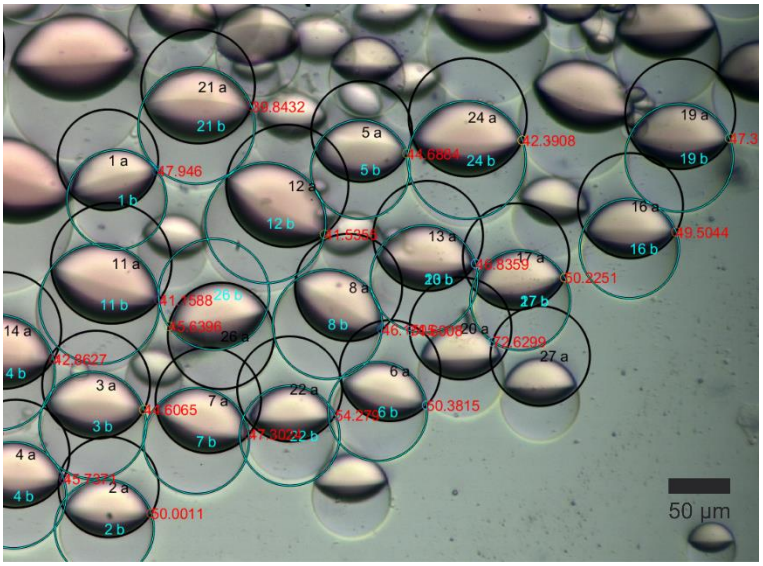

Figure S1. Sideview Image of complex emulsions, processed with the droplet curvature-analyzing algorithm.

1.5 Contact Angle Determination

Contact angles at the three-phase contact line of Janus particles were determined from side view images taken with the custom sideview setup. All studied droplets appeared overall to be spherical as a result of the ultralow interfacial tension between the aqueous phases. As a result, we used the contact angle θ (see also Figure 2A of the manuscript) as the sole parameter to quantitatively describe the morphology of the Janus droplets. For the determination of the contact angle, side view images of the droplets were analyzed using the above-described image-processing algorithm.

1.6 Pendant Drop Tensiometry

Interfacial tension measurements were performed on a drop shape analyzer tensiometer (DSA10-MK2, Krüss) in the pendant drop configuration. A CCD camera recorded the image of the drop. To obtain values of the surface tension, the drop profiles were fitted to the Laplace equation. The interfacial tension decreased exponentially with time after the formation of the pendant drop because surfactant molecules continued to adsorb at the droplets interface. To keep the results comparable and to take the exponential decline of the interfacial tension into consideration, we monitored the process over time. Therefore we have taken the interfacial tension values when the rate of decrease was slower than 0.2 mN/m per 30 seconds.

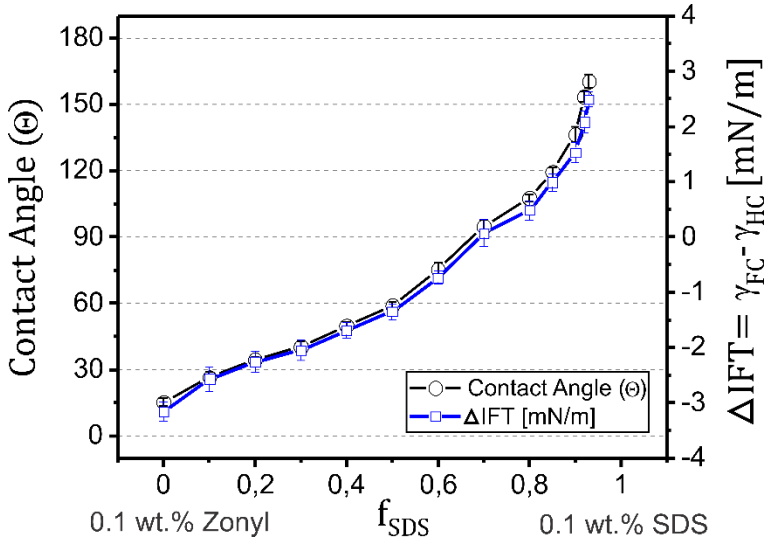

Figure S2. Droplet morphology diagram for the heptane-perfluorodecalin-water system showing the contact angle (θ) and ΔIFT= γ_{FC} - γ_{HC} as a function of the fraction of 0.1 wt.% SDS, f_{SDS}, where the other fraction is 0.1 wt.% Zonyl FS-300. The reconfiguration of the droplet morphology coincides with ΔIFT at varying surfactant fractions.

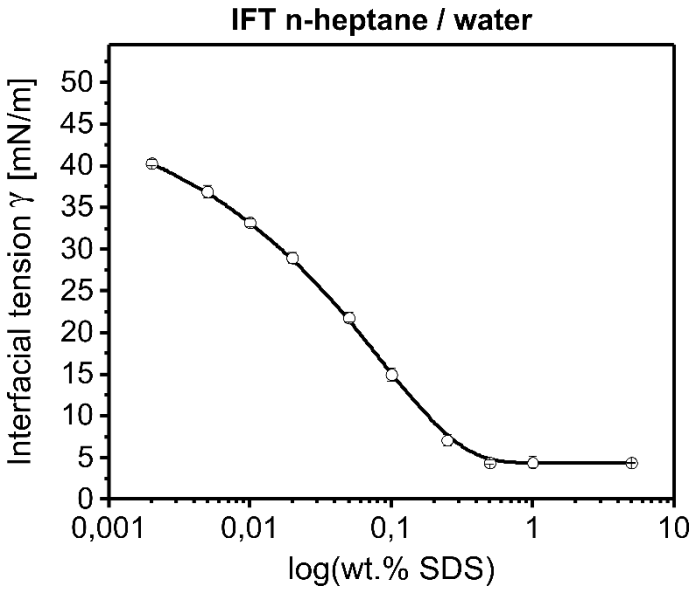

Figure S3. Interfacial tension of the n-heptane-water interface at different concentrations of SDS, measured with the Pendant Drop Method. The Interfacial Tension γ is decreasing until the CMC of SDS is reached (~0.237 wt.% (Responsive Drop method)).

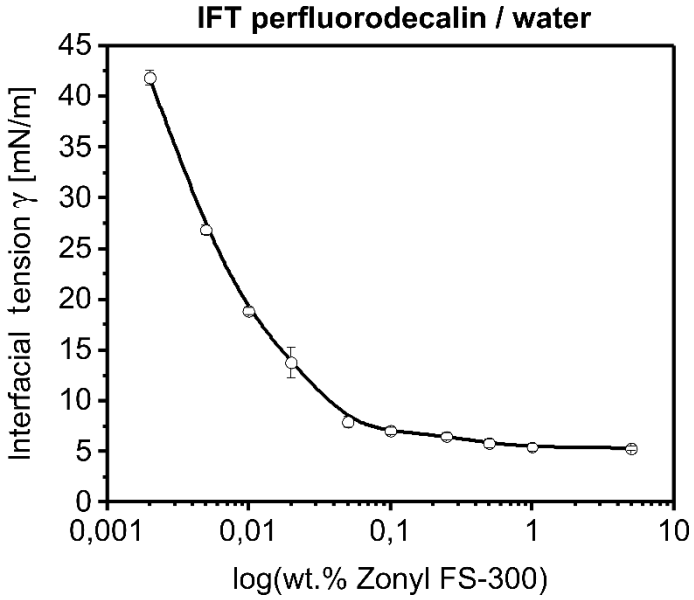

Figure S4. Interfacial tension of the perfluorodecalin-water interface at different concentrations of Zonyl FS-300, measured with the Pendant Drop Method. The Interfacial Tension γ is decreasing until the CMC of Zonyl FS-300 is reached (~0.115 wt.% (Responsive Drop method)).

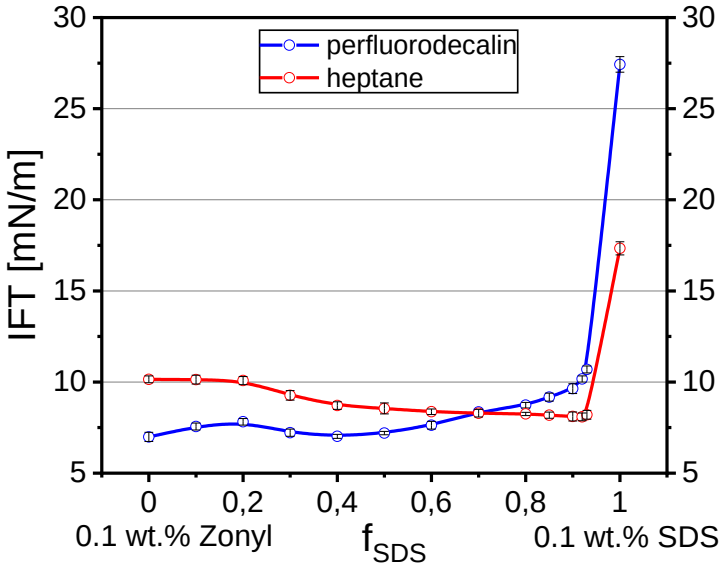

Figure S5. Interfacial tension of the perfluorodecalin-water- and the n-heptane-water interface as a function of the fraction of 0.1 wt.% SDS, f_{SDS}, where the other fraction is 0.1 wt.% Zonyl FS-300. At the crossing point of the two interfacial tensions ($\gamma_{FC} = \gamma_{HC}$) the droplets assume a perfect Janus state.

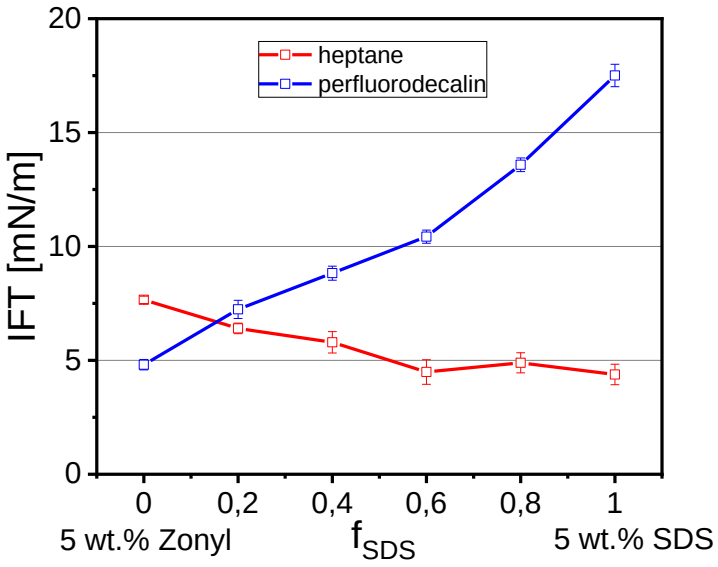

Figure S6. Interfacial tension of the perfluorodecalin-water- and the n-heptane-water interface as a function of the fraction of 5 wt.% SDS, f_{SDS}, where the other fraction is 5 wt.% Zonyl FS-300.

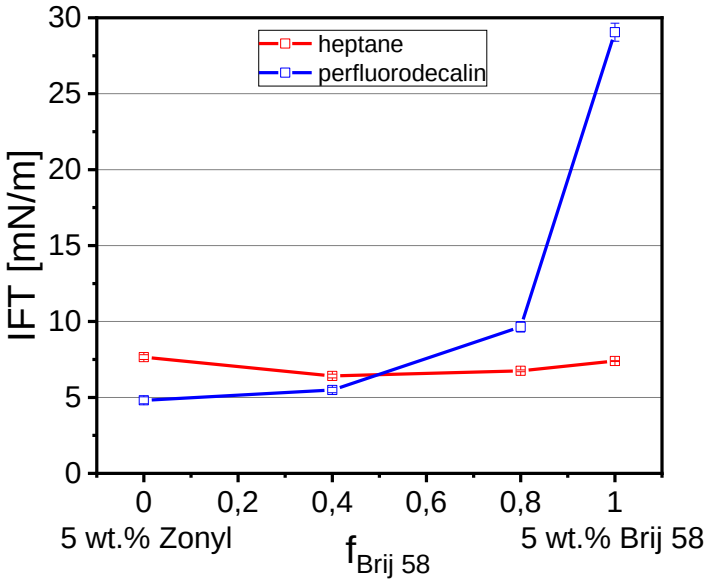

Figure S7. Interfacial tension of the perfluorodecalin-water- and the n-heptane-water interface as a function of the fraction of 5 wt.% Brij 58, $f_{Brij\ 58}$, where the other fraction is 5 wt.% Zonyl FS-300.

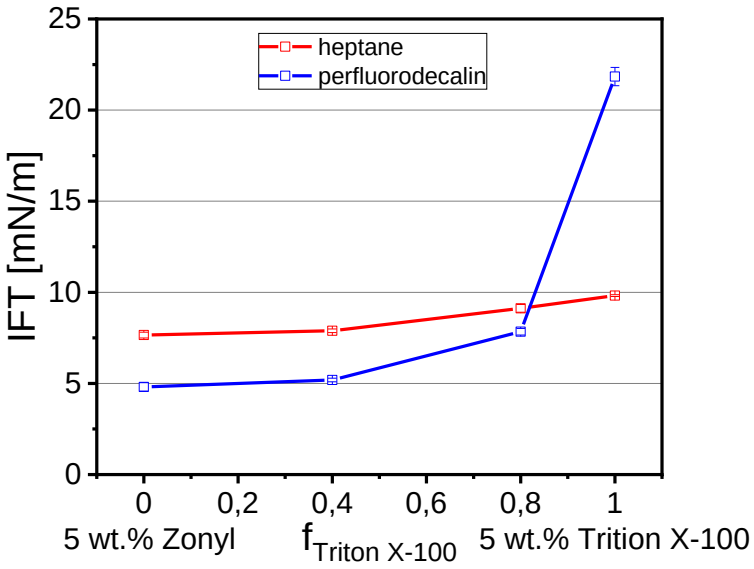

Figure S8. Interfacial tension of the perfluorodecalin-water- and the n-heptane-water interface as a function of the fraction of 5 wt.% Trition X-100, $f_{Triton\ X\text{-}100}$, where the other fraction is 5 wt.% Zonyl FS-300.

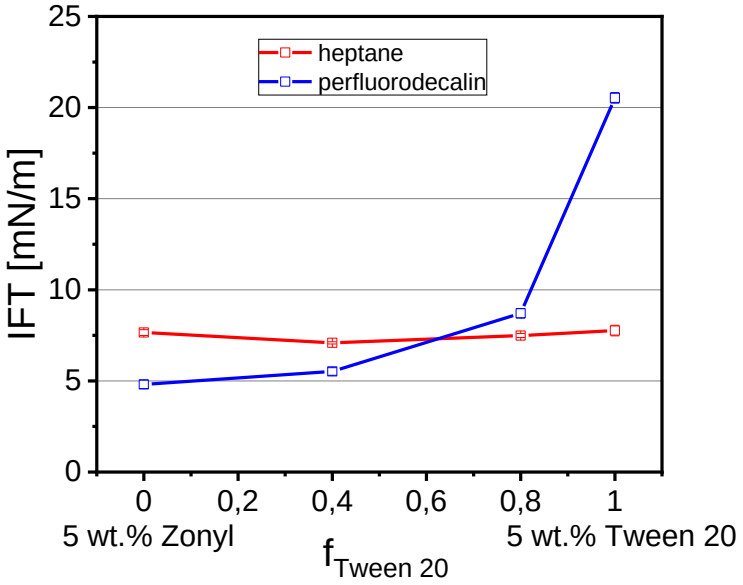

Figure S9. Interfacial tension of the perfluorodecalin-water- and the n-heptane-water interface as a function of the fraction of 5 wt.% Tween 20, $f_{Tween\ 20}$, where the other fraction is 5 wt.% Zonyl FS-300.

2 Droplet Fabrication

The complex emulsions in this work were prepared by a one-step temperature-induced phase-separation method. The inner oil phase consisted of n-heptane dyed with Sudan Red 7B and perfluorodecalin in a 1:1 ratio. The continuous aqueous phase consisted of distilled water mixed with various concentrations of the following surfactants: AOT, AzoTAB, Brij 58, CTAB, SDS, Triton X-100, Tween 20 and Zonyl FS-300. For each Emulsion 100 µL of the heptane-perfluorodecalin mixture was heated above the upper critical solution temperature (UCST) and added to 1 mL of a preheated aqueous surfactant solution. The resulting mixture was emulsified subsequently by using a vortex mixer (10 s, 2500 rpm, Vortex Genie 2, scientific industries). The prepared complex emulsions were allowed to cool down to room temperature before imaged.

3 CMC and γ_{HC}^{*} Determination with the Dynamic Drop Method

To determine the surfactants CMC and γ_{HC}^{*} values we measured the droplets contact angle at different hydrocarbon surfactant concentrations and kept the fluorocarbon surfactant (Zonyl FS-300) concentration constant, close to its CMC (Figure S10). The constant fluorocarbon surfactant concentration acted as an internal standard and served to maintain overall droplet stability. Initially, the droplet contact angle increased rapidly with an increasing amount of hydrocarbon surfactant until the CMC was reached. After the CMC the slope of the contact angle change was significantly lower. To extract the surfactants' CMC and γ_{HC}^{*} values from the droplet morphology diagram we used the linear fit functions describing the two different areas where the slope of the droplets contact angle change differ from each other. The CMC value was extracted from the crossing point of the two linear fit functions. The corresponding y-value describing the droplet contact angle at the surfactant CMC (measured against a constant fluorocarbon surfactant concentration) was then translated into an interfacial tension value using the function of the linear fit from Figure 2B of the manuscript. The contact angle is directly proportional to the quantity $\gamma_{FC} - \gamma_{HC}$. With the function describing the linear fit of Figure 2B in the main manuscript at hand ($\theta = 26.41 * (\gamma_{FC} - \gamma_{HC}) + 95.02$), and knowing the quantity of γ_{FC} at the particular fluorocarbon surfactant concentration, the respective γ_{HC} value could be calculated (Table 1).

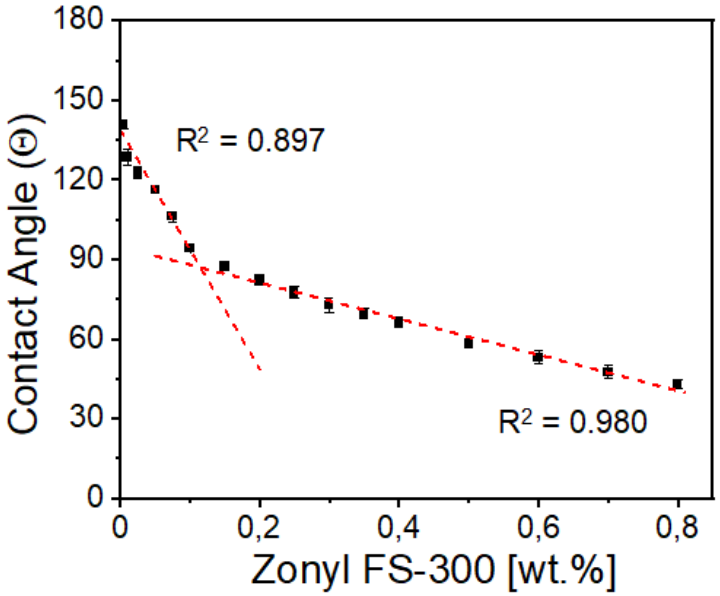

Figure S10. Droplet morphology diagram measured against different concentrations of Zonyl-FS300. We kept the SDS concentration constant at 1 wt.%. The CMC of Zonyl FS-300 determined with the Responsive Drop Method is at ~0.115 wt.%.

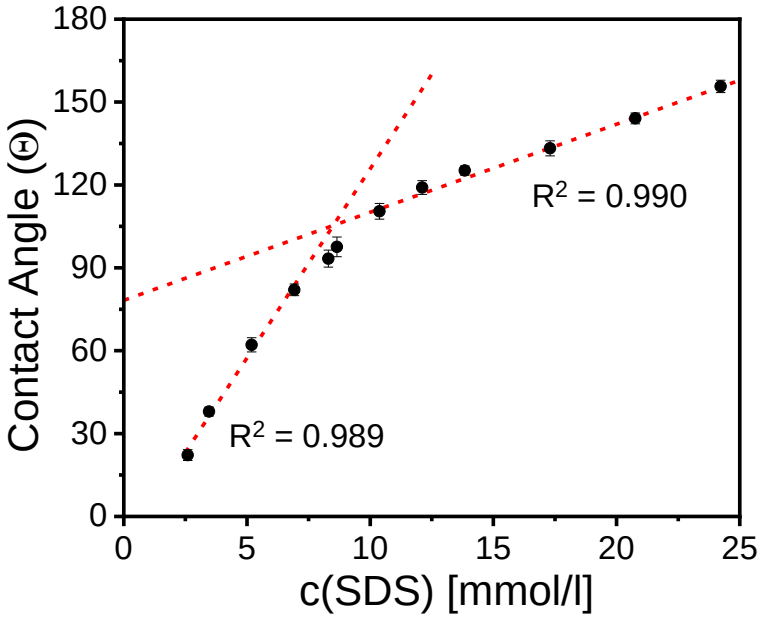

Figure S11. Droplet morphology diagram measured against different concentrations of SDS. We kept the Zonyl FS-300 concentration constant at 1 wt.%.

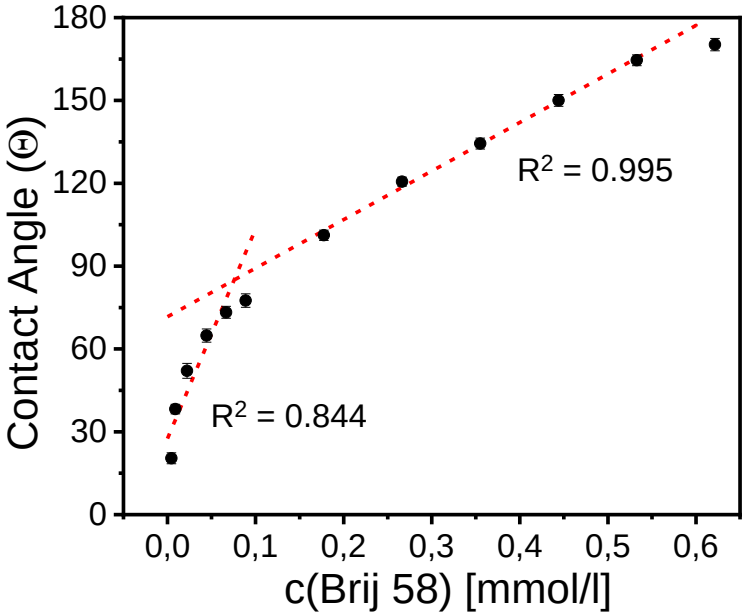

Figure S12. Droplet morphology diagram measured against different concentrations of Brij 58. We kept the Zonyl FS-300 concentration constant at 0.025 wt.%.

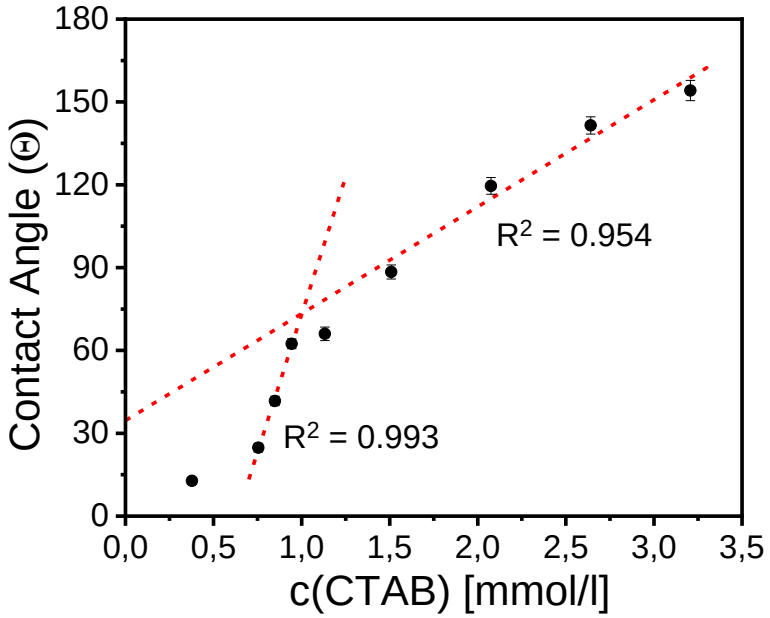

Figure S13. Droplet morphology diagram measured against different concentrations of CTAB. We kept the Zonyl FS-300 concentration constant at 0.25 wt.%.

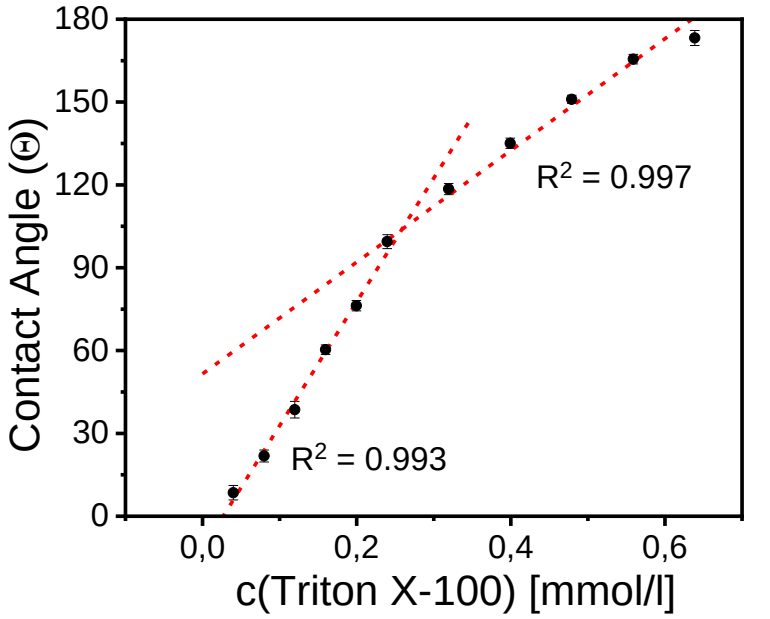

Figure S14. Droplet morphology diagram measured against different concentrations of Triton X-100. We kept the Zonyl FS-300 concentration constant at 0.05 wt.%.

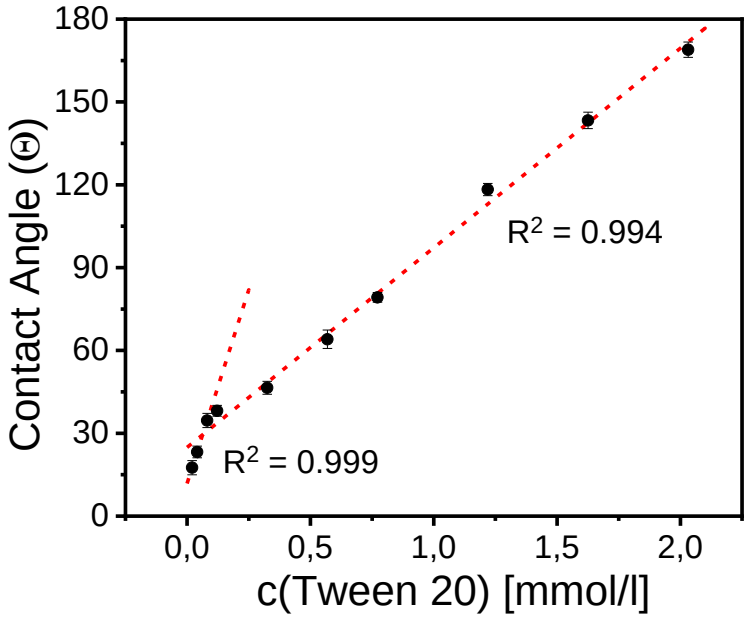

Figure S15. Droplet morphology diagram measured against different concentrations of Tween 20. We kept the Zonyl FS-300 concentration constant at 0.025 wt.%.

4 Light-responsive surfactant: AzoTAB

4.1 Synthesis of AzoTAB

1) 4-butyl-4'-hydroxyazobenzene

15 g (100.5 mmol, 1 eq.) of 4-butylanilin was dissolved in 60 mL of HCl (5 M) at 0 °C. Then 6.934 g (100.5 mmol, 1 eq.) of sodium nitrite in 15 mL of water was added. The reaction mixture was left to react for 1 h at 0 °C. Then 9.458 g (100.5 mmol, 1 eq.) of Phenol and 29.279 g (251.3 mmol, 2.5 eq.) of sodium carbonate in 50 mL water was added. The product was precipitated as a brown solid. The reaction solution was filtered and the product was recrystallized in n-hexane. Then the product was dissolved in acetone and filtered again to separate the NaCl.

Yield: 18.997 g (74 %).

^{1}H-NMR (400 MHz, $CDCl_3$): 0.94 (t, 3H), 1.38 (m, 2H), 1.64 (m, 2H), 2.68 (t, 2H), 6.93 (d, 2H), 7.30 (d, 2H), 7.78 (d, 2H), 7.85 (d, 2H).

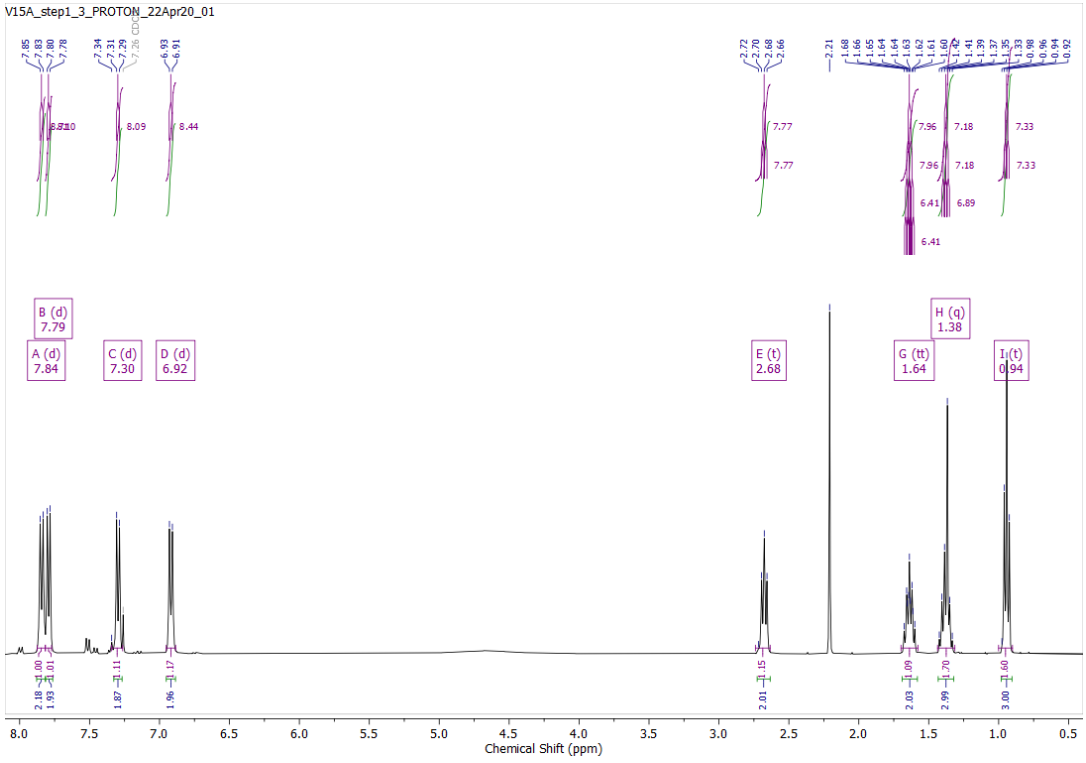

Figure S16. ^{1}H-NMR Spectra of 4-butyl-4'-hydroxyazobenzene.

2) 4-butyl-4'-(3-bromopropxy)azobenzene

18.997 g of 4-butyl-4'-hydroxyazobenzene (74.7 mmol, 1 eq.) in 100 mL THF was added dropwise into a mixture of 5.029 g potassium hydroxide (89.64 mmol, 1.2 eq.) and 8.38 mL of 1,3-dibromopropane (82.17 mmol, 1.1 eq.). The reaction was refluxed overnight. The crude was filtered to remove the KBr and then evaporated down to an oily solution that was resuspended in n-hexane for precipitation at low temperature. The precipitate was recrystallized and the hot solution was filtered to remove the solid dimer.

Yield: 8.210 g (29 %)

^{1}H-NMR (400 MHz, $CDCl_3$): 0.94 (t, 3H), 1.38 (m, 2H), 1.64 (m, 2H), 2.36 (m, 2H), 2.68 (t, 2H), 3.63 (t, 2H), 4.20 (t, 2H), 7.03 (d, 2H), 7.31 (d, 2H), 7.84 (d, 2H), 7.95 (d, 2H).

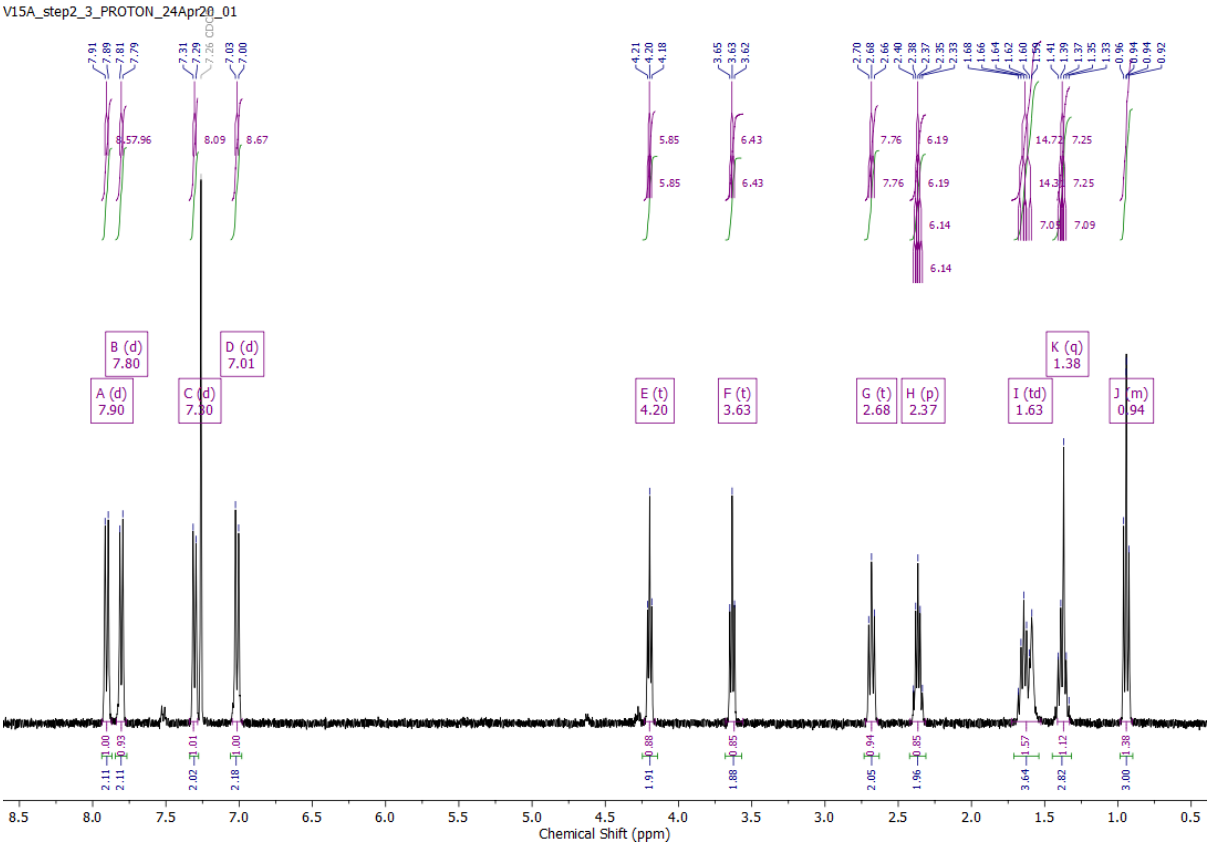

Figure S17. ^{1}H-NMR Spectra of 4-butyl-4'-(3-bromopropxy)azobenzene.

3) 4-butyl-4'-(3-trimethylammoniumpropoxy)phenylazobenzene (AzoTAB)

8 g of 4-butyl-4'-(3-bromopropxy)azobenzene (21.3 mmol, 1 eq.) was dissolved in 120 mL of ethylacetate and 180 mL of ethanol at 70 °C. 20.36 mL of trimethylamine (35 % in ethanol, 85.3 mmol, 4 eq.) was added dropwise. The reaction was refluxed for 48 h. Upon cooling to RT a precipitate of AzoTAB forms. The precipitate was filtered and recrystallized in a 90:10 v/v mixture of ethylacetate and ethanol.

Yield: 6.631 g (88 %, overall yield: 19 %)

^{1}H-NMR (400 MHz, $CDCl_3$): 0.93 (t, 3H), 1.37 (m, 2H), 1.63 (m, 2H), 2.34 (m, 2H), 2.67 (t, 2H), 3.49 (s, 9H), 3.90 (t, 2H), 4.20 (t, 2H), 7.00 (d, 2H), 7.29 (d, 2H), 7.80 (d, 2H), 7.89 (d, 2H).

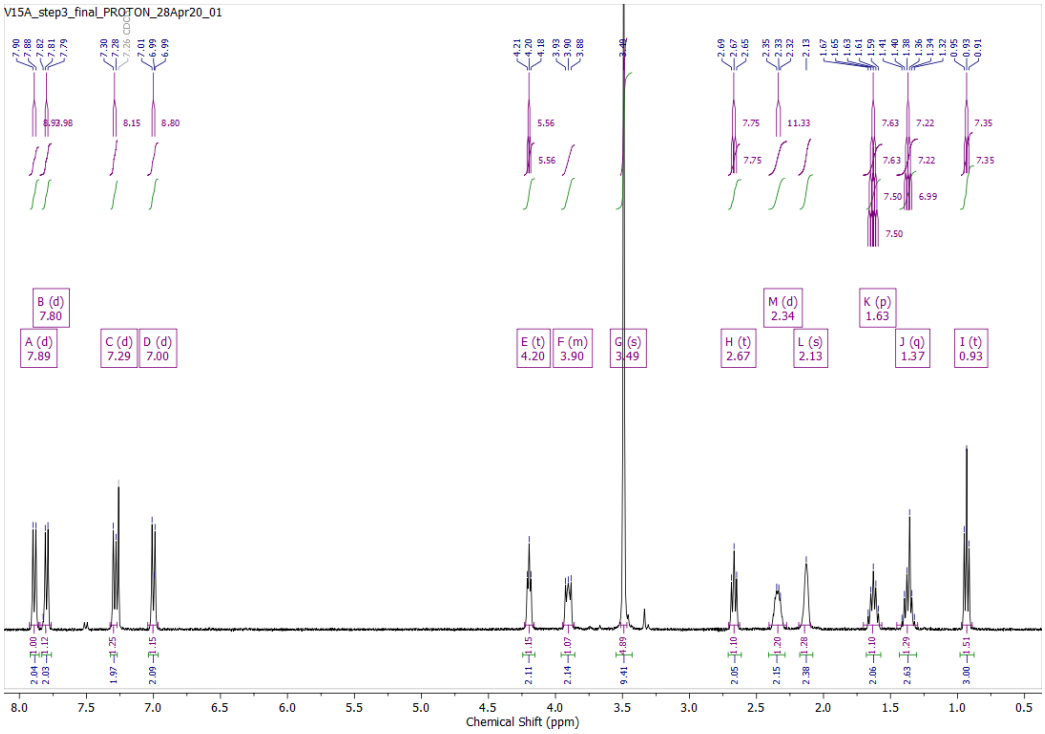

Figure S18. ^{1}H-NMR Spectra of 4-butyl-4'-(3-trimethylammoniumpropoxy)phenylazobenzene (AzoTAB).

4.2 Supporting Video

Supporting Video V1. Reversible morphological response of AzoTAB stabilized Janus emulsions in response to UV and blue light.

5 Reference

[1] . L. Zeininger, S. Nagelberg, K. S. Harvey, S. Savagatrup, M. B. Herbert, K. Yoshinaga, J. A. Capobianco, M. Kolle, T. M. Swager, *ACS Cent. Sci.* 2019**, *5***, 789-795.